Journal of Sound and Vibration 326 (2009) 709–724

Contents lists available at ScienceDirect

Journal of Sound and Vibration

journal homepage: www.elsevier.com/locate/jsvi

Vibration analysis of beams with open and breathing cracks subjected to moving masses

A. Ariaei, S. Ziaei-Rad *, M. Ghayour

Department of Mechanical Engineering, Isfahan University of Technology, Isfahan, Iran

ARTICLE INFO

Article history:
Received 18 November 2007
Received in revised form
3 May 2009
Accepted 5 May 2009
Handling Editor: S. Bolton
Available online 7 June 2009

ABSTRACT

This paper presents an analytical approach, as well as a calculation method for determining the dynamic response of the undamped Euler–Bernoulli beams with breathing cracks under a point moving mass using the so-called discrete element technique (DET) and the finite element method (FEM). First, the standard DET formulation is modified to consider the effects of Coriolis and centrifugal forces. Next, the formulation is extended to be able to evaluate the cases with open and breathing cracks under moving masses. The results will be validated against those reported in the literature and also compared with results from the finite element method. The effects of the moving mass velocity, location, and size of the crack on beam deflection will be investigated. Natural frequencies of the beam under the effect of crack will also be studied to compare the results with those of a beam without crack. It is observed that the presence of crack results in higher deflections and alters beam response patterns. In particular, the largest deflection in the beam for a given speed takes longer to build up, and a discontinuity appears in the slope of the beam deflected shape at the crack location. The effects of crack and load depend on speed, time, crack size, crack location, and the moving mass level.

1. Introduction

Crack is one of the most common defects in structures that may result in adverse effects on the behaviour and ill performance of structures, which can eventually lead to their collapse. Typically, cracks induce changes in the structure's stiffness, also reducing its natural frequency. Moreover, the crack will open and close in time depending on loading conditions and vibration amplitude. The static deflection due to some loading component on the cracked beam (residual loads, body weight of a structure, etc.) combined with the vibration effect may cause the crack to open at all times, to open and close regularly, or to close completely depending on various loads at a given time.

If the static deflection due to some loading component on the beam such as dead loads, own weight, etc. is larger than the vibration amplitudes, then the crack remains open all the time. If the static deflection is small, then the crack will open and close in time depending on the vibration amplitude. Various studies over the last decade have indicated that a beam with a breathing crack, i.e., one which opens and closes during oscillation, shows nonlinear dynamic behaviour because of the variation in the structural stiffness which occurs during the response cycle.

On the other hand, the effect of moving loads and masses on structures and machines is an important problem both in the field of transportation and in the design of machining processes. A moving load (or moving mass) produces larger

* Corresponding author. Tel.: +98 311 3915244; fax: +98 311 3912628.
E-mail address: szrad@cc.iut.ac.ir (S. Ziaei-Rad).

0022-460X/$ - see front matter © 2009 Elsevier Ltd. All rights reserved.
doi:10.1016/j.jsv.2009.05.013

Nomenclature

a	depth of the crack
A	cross sectional area
$\mathbf{A}$	stiffness matrix of the beam
b	height of the beam
$\mathbf{C}$	damping matrix related to Coriolis force
D	crack compliance
E	Young's modulus
EI	bending stiffness of the beam
h	length of element
$\mathbf{H}$	inertia matrix related to inertia force
I	beam cross section moment of inertia
I^*	beam central mass moment of inertia
$\mathbf{K}$	stiffness matrix related to centrifugal force
K_j	rotational stiffness of joint j
L	length of the beam
L_c	distance of crack from right hand side of the beam
m	mass per unit length
m^*	mass of an element
M_j	bending moment of joint j
n	number of elements of the beam
p_j	generalized load on the jth element
$\mathbf{Q}$	mass matrix of the beam
S_r	reduced cross section
T	kinetic energy of the beam
T_0	time needed for travelling of the moving mass across the beam
v	velocity of the moving load
V	potential energy of the beam
$\mathbf{W}$	weight matrix of the moving mass
$\mathbf{Y}$	deflection matrix of the beam
y^*	deflection of element centre
$\bar{z}$	radius of gyration
δ_i	boundary condition parameters
θ	relative rotation of the attached bars
ρ	density of the beam
Ψ	mechanical energy of the beam
ω_j	angular velocity of jth element
I	index related to the beam
p, II	indexes related to the moving mass

deflections and higher stresses than does an equivalent load applied statically. These deflections and stresses are functions of both time and speed of the moving loads. It is, therefore, essential to detect and control damages in structures subjected to a moving mass. Very few studies have been reported in the literature that deal with moving load or moving mass problems under the effect of cracks.

For more than a century, the analysis of continuous elastic systems subjected to moving masses has been the subject of interest in many diverse fields such as civil and aerospace engineering [1]. Historically, the problem first arose in the design of railway bridges, and later in other transportation engineering problems such as the design of bridges, guideways, overhead cranes, cableways, rails, roadways, runways, tunnels, and pipelines with moving masses [2]. There have been numerous investigations in this regard. Some of the early investigations were by Stokes [1] and Ayre [3]. There are two well-known monographs in this area, one by Inglis [4] and the other by Hillerborg [5]. A more recent book by Fryba [6] includes analyses of moving masses on a beam under different loading conditions.

Cheng et al. [7] considered the vibration response of a beam with breathing crack. A cantilever beam was used and modelled as a one-degree-of-freedom lumped parameter system. This simplified model simulates the beam vibrating at its first mode. They incorporated the breathing crack model into a single-degree-of-freedom system as a harmonic change in the beam stiffness. Their analysis showed that the natural frequency reduction for a fatigue crack (breathing crack) was much smaller than that for an open crack. This means that fatigue cracks would be more difficult to recognize by frequency monitoring and that crack detection by an open crack model would underestimate the crack severity if it were actually growing under fatigue loading conditions.

Pungo et al. [8] presented a technique capable of evaluating the dynamic response of a beam with several breathing cracks perpendicular to its axis and subjected to harmonic excitation. The method described is based on the assumption of periodic response and that cracks open and close continuously. Their results showed that the presence of breathing cracks in a beam under harmonic excitation results in nonlinear dynamic behaviour which gives rise to superharmonics in the spectrum of the response signals, the amplitude of which depends on the number, location, and depth of any cracks present.

Kisa and Brandon [9] developed a finite element scheme for computing the eigensystem for a cracked beam for different degrees of closure. In their study, the finite element method (FEM), the component mode synthesis method, and the linear elastic fracture mechanics theory are integrated for modelling cracked structures.

Chondros and Dimarogonas [10] studied vibration of a simply supported Euler–Bernoulli continuous cracked beam. For a beam with a breathing crack, they assumed it to be a piecewise linear system. In other words, the bilinear-type breathing crack has only two states, either fully open or fully closed. They concluded that the changes in vibration frequencies for a fatigue-breathing crack are smaller than the ones caused by open cracks.

Douka and Hadjileontiadis [11] investigated the dynamic behaviour of a cantilever beam with a breathing crack both theoretically and experimentally. The main aim of their work was to reveal the nonlinear behaviour of the system by using time frequency methods. A simple single-degree-of freedom lumped system was employed to simulate the dynamic behaviour of the beam and a simple periodic stiffness model was used to model the breathing crack.

Bovsunovsky and Surace [12] developed a mathematical model of a beam with a closing crack which takes into account the relationship between the energy dissipated in a crack and the nominal stress intensity factor range. For the breathing of the crack, they used a simple fully open or fully closed crack. They verified some of the results by experimental data.

Abraham and Brandon [13] proposed a technique based on a hybrid approach using mode superposition when a cracked structure was in either the open-crack or closed-crack condition but adopting a time-domain approach during the brief intervals of transition.

Akin and Mofid [14,15] developed the so-called discrete element technique (DET) for the vibration analysis of Euler–Bernoulli beams subjected to a concentrated moving mass. Mofid [16] extended the technique to analyse the dynamic behaviour of beams on elastic foundations. The response of beams with internal hinges was investigated by Mofid and Shadnam [17]. They used the DET to formulate moving mass carrying beams with internal hinges and with variable boundary conditions. They also verified their solutions by comparing them against a general-purpose nonlinear dynamic finite element program. Yavari et al. [18] extended the work of Mofid to a case with lumped masses and Timoshenko beams, i.e., they were able to consider the effect of shear deformation and rotary inertia and Ziaei et al. [19] studied a Timoshenko beam under uniform partially distributed moving masses.

There has been growing interest in studying the vibration of cracked components and structures. The presence of cracks in a structure introduces local flexibility and, therefore, alters the dynamic response of the structure. In one estimate, over 500 papers on this subject were published in two decades [20]. Recent investigations in this area include beams with multiple cracks [21], effect of cracks on rotating bladed disks [22], and nonlinear response of a beam with a number of breathing cracks [23]. Interest in the dynamic analysis of damaged beams has been ongoing for the past 40 years, particularly because of its relationship to the automatic monitoring of structural integrity.

Very few studies have been reported in the literature on the effect of cracks on moving load or moving mass problems. Parhi and Behera [24] used the Runge–Kutta method to determine the deflection of a cracked circular shaft subjected to a moving mass. Recently, Mahmoud [25] used an equivalent static load approach to determine the stress intensity factors for a single- or a double-edge crack in a beam subjected to a moving load.

Mahmoud and Abou zaid [26] studied the dynamic response of a beam with a crack subjected to a moving mass. The aim was to determine the effect of transverse cracks on the dynamic behaviour of simply supported undamped Bernoulli–Euler beams subject to a moving mass. They used the approximate stationary mass (SM) approach recommended by Fryba [6] for light moving masses. They did not take into account the Coriolis and centrifugal forces due to the moving mass. They also considered an open crack and modelled the effect of crack by a rotational spring connecting two undamaged beam segments. They concluded that open crack presence resulted in higher deflections and altered the beam response patterns. In particular, the largest deflection in the beam for a given speed takes longer to build up, and a discontinuity appears in the slope of the beam-deflected shape at the crack location.

Yoon and Son [27] studied the effect of an open crack and a moving mass on the dynamic behaviour of a simply supported pipe conveying fluid. This was a circular hollow cross section and the crack was assumed to be always open during vibrations. They derived the equation of motion by using Lagrange's equation and used the numerical method to analyse it. The crack section is represented by a local flexibility matrix connecting two undamaged pipe segments; that is, the crack is modelled as a rotational spring.

Bilello and Bergman [28] carried out a theoretical and experimental study of the response of a damaged Euler–Bernoulli beam traversed by a moving mass. Damage was modelled in their study through rotational springs whose compliance is evaluated using linear elastic fracture mechanics. They calculated the response of the system by using the transfer matrix method, taking into account the effective mass distribution of the beam. They also validated their analytical solution by a series of experimental tests. Their results indicate that the experimental response is often larger than the calculated one.

To the authors' best knowledge, all the above papers considered beams with moving load and open crack or beams with breathing cracks under harmonic forces. In this study, the DET will be first modified and then extended to consider effects of crack on the dynamic response of a beam subjected to a moving mass with arbitrary boundary conditions. Since fully open crack is a crude modelling for some systems, the breathing cracks formulation is presented and compared with the open crack formulation. An FE code with similar crack model is also developed and the results are compared with those from DET.

2. DET formulation for beams with open cracks

As shown in Fig. 1, it is assumed that the moving mass enters the beam from the left-hand support at time $t = 0$ at a constant velocity v. All displacements are assumed to be small and all initial conditions are taken as zero.

First, the DET solution of Mofid [18] is illustrated and then this formulation is extended to a beam with open and breathing cracks. The DET divides a continuous flexible beam into a system of rigid bars and joints, which resist relative rotation of the attached bars. Therefore, the kinetic energy is calculated for rigid bars and all potential energy is stored in flexible joints. Some shortcomings of the DET can be expressed as:

1. The formulation of the discrete element technique is much complicated than the standard finite element method.
2. The assumption that replacing the continuous flexible elements by a system of rigid bars and flexible joints made by DET leads to the discontinuities in bending slopes and moments at each flexible joint. However, by increasing the

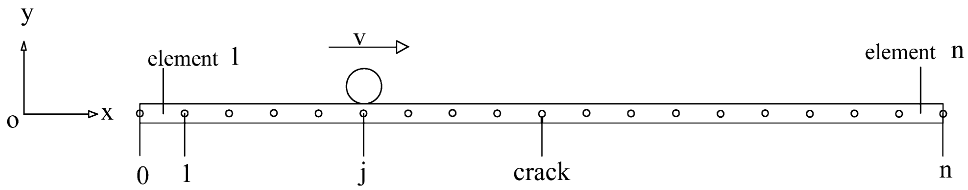

Fig. 1. Beam and moving mass.

number of rigid elements, the moment between adjacent joints decreases and hence a roughly uniform moment over a short length is reached. Thus, the results improve by increasing the number of rigid elements and converge to the exact solution as the number discrete elements increases. However, the numerical solution of these systems will be affected by additional discretizations and round-off errors.

The total energy of the system is equal to the energy of the beam plus the energy of the moving load. We will consider only the bending deflections of the beam. Following the notation of [19], we define three parameters δ_i, $i = 1,2,3$ for different types of boundary conditions. δ_1 corresponds to the boundary condition on the left hand side of the beam while δ_2 and δ_3 define the boundary conditions on the right hand side of it. The actual values of these parameters can be either 1 or 0 [18,19].

To use Lagrange's equations, the kinetic and potential energy of the system should be determined. For the bending deflection, the total kinetic energy of the beam can be expressed as the sum of the translational and rotational components [19]:

$$T_\mathrm{I} = \frac{1}{2}\sum_{j=1}^{n} m_j^* \left(\frac{\mathrm{d}y_j^*}{\mathrm{d}t}\right)^2 + \frac{1}{2}\sum_{j=1}^{n} I_j^* \omega_j^2 \tag{1}$$

where n is the number of elements, m^* the mass of the element, I^* the mass moment of inertia at the centre of the element, and y^* the deflection at the centre of each element. The deflection, the moment of inertia, and the rotational velocity can be approximated as

$$y_j^* = \tfrac{1}{2}(y_{j-1} + y_j) \tag{2a}$$

$$I_j^* = \rho I h + \rho A \frac{h^3}{12} \tag{2b}$$

$$\omega_j = \frac{1}{h}(\dot{y}_j - \dot{y}_{j-1}) \tag{2c}$$

where h is the length of the element, ρ the density of the beam, A the cross sectional area, and I the constant cross section moment of inertia.

The potential energy of the beam due to bending is given by

$$U_I = \frac{1}{2}\sum_{j=1}^{n} M_j\theta_j = \frac{1}{2}\sum_{j=1}^{n} K_j\theta_j^2 \tag{3}$$

$$\theta_j = \frac{1}{h}[(y_j - y_{j-1}) + (y_j - y_{j+1})]$$

where

$$M_j = K_j\theta_j, \quad K = \frac{EI}{h}, \quad m_j^* = mh, \quad h = \frac{L}{n} \tag{4}$$

Here, L is the length of the beam, m the mass per unit length, and EI the bending stiffness, M_j and K_j are the bending moment and the rotational stiffness of joint j, and θ the relative rotation of the attached bars. The term for rotational stiffness of joint j is correct only if the element $j-1$ does not have a crack. In other words, if the element $j-1$ has a crack, the rotational stiffness of joint j should be calculated separately. In that case, the rotational stiffness of joint j can be written as [26]

$$\theta_j = \theta_{j0} + DM_j \tag{5}$$

where θ_j is the relative rotation of joint j in the presence of a crack, θ_{j0} the relative rotation of joint j if the crack was absent, D the crack compliance, and M_j the bending moment at joint j. The crack compliance D may be determined by modelling the cracked section as a rotational spring connecting two undamaged beam segments. The stiffness of the rotational spring is determined using fracture mechanics and is incorporated into the m-matrix approach [26]. In this study, an expression for D was derived by using the results from [26] which for a rectangular section of height b with a crack of depth a, it can be shown to be

$$D = \frac{2b}{EI}\left(\frac{a/b}{1-a/b}\right)\{5.93 - 19.69(a/b) + 37.14(a/b)^2 - 35.84(a/b)^3 + 13.12(a/b)^4\} \tag{6}$$

Using Eq. (5), the rotational stiffness at joint j can be calculated as

$$k_j = \beta_j k_{j0} \tag{7}$$

where k_j is the rotational stiffness of joint j in the presence of a crack, k_{j0} the rotational stiffness of joint j if the crack was absent, and β_j, that is only related to joint j, is equal to

$$\beta_j = \frac{1}{1 + Dk_{j0}} \tag{8}$$

For calculating the potential energy of the beam, the rotational stiffness of elements with crack should be determined by (7) and then replaced in (3).

The work carried out by the external forces, or the minus of the potential energy of generalized loading, is given by

$$\Omega_1 = \sum_{j=1}^{n-1} p_j y_j + \delta_3 p_n y_n \tag{9}$$

where p_j is the generalized load acting on the jth element. The last term in (9) is the effect of the boundary condition on the right hand side of the beam. For the free boundary condition case, the value of δ_3 is unity [18,19].

The potential energy of the beam is

$$V_{\mathrm{I}} = U_{\mathrm{I}} - \Omega_{\mathrm{I}} \tag{10}$$

The total mechanical energy of the beam is the sum of kinetic and potential energies:

$$\Psi_{\mathrm{I}} = T_{\mathrm{I}} + V_{\mathrm{I}} = T_{\mathrm{I}} + U_{\mathrm{I}} - \Omega_{\mathrm{I}} \tag{11}$$

Let us define the moment of inertia of the beam area as the product of the area and the square of gyration radius of the beam's section about z-axis:

$$I = A\bar{z}^2 \tag{12}$$

By substituting Eq. (12) in Eq. (2), we have

$$I_j^* = \frac{mh^3}{12}\left(1 + \frac{12\bar{z}^2}{h^2}\right) \tag{13}$$

Now the kinetic and potential energy of the beam can be written as

$$T_{\mathrm{I}} = \left(\frac{mL}{6n}\right)\left(1 + 3\frac{\bar{z}^2}{h^2}\right)\left[2\sum_{j=1}^{n-1}\dot{y}_j^2 + \delta_3\dot{y}_n^2\right] + \left(\frac{mL}{6n}\right)\left(1 - \frac{6\bar{z}^2}{h^2}\right)\left[\sum_{j=1}^{n-2}\dot{y}_j\dot{y}_{j+1} + \delta_3\dot{y}_{n-1}\dot{y}_n\right] \tag{14}$$

$$V_{\mathrm{I}} = \frac{EIn^3}{2L^3}\left\{2\delta_1(y_1)^2 + (2y_1 - y_2)^2 + \sum_{j=2}^{r-1}(2y_j - y_{j-1} - y_{j+1})^2 + \beta_r(2y_r - y_{r-1} - y_{r+1})^2 \right.$$
$$\left. + \sum_{r+1}^{n-2}(2y_j - y_{j-1} - y_{j+1})^2 + (-y_{n-2} + 2y_{n-1} + \delta_3 y_n)^2 + 2\delta_2(-y_{n-1} + \delta_3 y_n)^2\right\} - \sum_{j=1}^{n-1} p_j y_j - \delta_3 p_n y_n \tag{15}$$

In Eq. (15), only one crack has been considered at element $r-1$ but if the number of cracks was more than one, the coefficient β_j would have to be considered for all related terms in this equation in the same manner.

Now, we need to obtain kinetic and potential energy expressions for a moving mass. The kinetic energy related to the linear moving mass speed is omitted from the kinetic energy at this stage. Its effect will be considered later in calculating the Coriolis and centrifugal forces. Therefore, the kinetic energy of the moving mass only related to the inertia force, at any instant, can be written as

$$T_{\mathrm{II}} = 0, \quad 0 < t_0 < \frac{L}{2nv}$$

$$T_{\mathrm{II}} = \frac{1}{2}m_p\left(\frac{\mathrm{d}y_j}{\mathrm{d}t}\right)^2, \quad \frac{(2j-1)L}{2nv} < t_j < \frac{(2j+1)L}{2nv}$$

$$T_{\mathrm{II}}=\frac{1}{2}\delta_3 m_p\left(\frac{\mathrm{d}y_n}{\mathrm{d}t}\right)^2,\quad \frac{(2n-1)L}{2nv}<t_n<\frac{L}{v}\tag{16}$$

The potential energy of the moving mass is given by

$$V_{\mathrm{II}}=0,\quad 0<t_0<\frac{L}{2nv}$$

$$V_{\mathrm{II}}=m_p g y_j,\quad \frac{(2j-1)L}{2nv}<t_j<\frac{(2j+1)L}{2nv}$$

$$V_{\mathrm{II}}=m_p g\delta_3 y_n,\quad \frac{(2n-1)L}{2nv}<t_n<\frac{L}{v}\tag{17}$$

The general dynamic equation can now be obtained from Lagrange's equations.

$$\left[\frac{\mathrm{d}}{\mathrm{d}t}\left(\frac{\partial T}{\partial \dot{y}_j}\right)+\left(\frac{\partial V}{\partial y_j}\right)\right]_{\mathrm{I}}+\left[\frac{\mathrm{d}}{\mathrm{d}t}\left(\frac{\partial T}{\partial \dot{y}_j}\right)+\left(\frac{\partial V}{\partial y_j}\right)\right]_{\mathrm{II}}=0\tag{18}$$

where (I) refers to the beam and (II) refers to the moving mass. The final equation may be obtained by substituting (14)–(17) into (18). After some rearrangement and by considering the effects of Coriolis and centrifugal forces (see Appendix A) to the DET formulation [29], a matrix equation of motion may be obtained at each instant:

$$(\mathbf{Q}+\mathbf{H})\mathbf{Y}_{,\mathbf{tt}}+\mathbf{C}\mathbf{Y}_{,\mathbf{t}}+(\mathbf{A}+\mathbf{K})\mathbf{Y}=\mathbf{W}+\mathbf{P}\tag{19}$$

where $\mathbf{Q}$ is the constant symmetric tri-diagonal matrix, $\mathbf{A}$ the constant symmetric penta-diagonal matrix, and $\mathbf{H}$ has a single time-dependent diagonal term matrix. $\mathbf{P}$ is the generalized loading vector and $\mathbf{W}$ is a vector of the moving mass weight. Matrix $\mathbf{C}$ is derived from Coriolis force and serves to reduce the excitation effect of the moving mass. Matrix $\mathbf{K}$ is derived from the centrifugal force that is normal to the deformed longitudinal axis of the beam. Its direction on the moving mass is towards the beam centre of curvature at any point. The opposite of this force is exerted on the beam. In the example of this paper, the curvature of the beam is upward and, therefore, the deflections of all points on the beam increase when the matrix $\mathbf{K}$ is accounted for in the calculations. The derivation of matrices $\mathbf{C}$ and $\mathbf{K}$ are given in Appendix A.

Rearranging Eq. (19) in the form of a matrix at an interior node j, we obtain

$$(\mathbf{Q}+\mathbf{H_j})\mathbf{Y}_{,\mathbf{tt}}+\mathbf{C_j}\mathbf{Y}_{,\mathbf{t}}+(\mathbf{A}+\mathbf{K_j})\mathbf{Y}=\mathbf{W_j}+\mathbf{P},\quad j=1,\ldots,n\tag{20}$$

where

$$\mathbf{Y^T}=\{y_1\;\; y_2\ldots\;\; y_n\},\quad \mathbf{Y^T_{,t}}=\{y_{1,t}\;\; y_{2,t}\;\;\cdots\;\; y_{n,t}\},$$

$$\mathbf{Y^T_{,tt}}=\{y_{1,tt}\;\; y_{2,tt}\;\;\cdots\;\; y_{n,tt}\}\tag{21}$$

One of the differences between the matrices introduced in Eq. (19) and those in Ref. [18] is the effects of Coriolis and centrifugal forces introduced into the DET formulation that can be seen in $\mathbf{C_j}$ and $\mathbf{K_j}$ matrices. Explicit expressions for matrices $\mathbf{C_j}$ and $\mathbf{K_j}$ are given in Appendix A and other matrices can be found in [19].

The crack only affects some components of matrix $\mathbf{A}$. By considering a crack in element r−1 (or joint r), matrix $\mathbf{A}$ will take the following form:

$$\mathbf{A}=\frac{EIn^3}{2L^3}\begin{array}{c}\begin{array}{cccccccccc} & & & & r-1 & r & r+1 & & & \end{array}\\ \left[\begin{array}{cccccccccc}
4\delta_1+10 & -8 & 2 & & & & & & & \\
-8 & 12 & -8 & 2 & & & & & & \\
2 & -8 & 12 & -8 & 2 & & & & & \\
 & \cdots & \cdots & \cdots & \cdots & \cdots & & & & \\
 & & \cdots & \cdots & 10+2\beta_r & -4-4\beta_r & 2\beta_r & & & \\
 & & & \cdots & -4-4\beta_r & 4+8\beta_r & -4-4\beta_r & 2 & & \\
 & & & & 2\beta_r & -4-4\beta_r & 10+2\beta_r & -8 & \cdots & \\
 & & & & & 2 & -8 & 12 & \cdots & 2\delta_3 \\
 & & & & & & \cdots & \cdots & 4\delta_2+10 & -4\delta_3(1+\delta_2) \\
 & & & & & & & 2\delta_3 & -4\delta_3(1+\delta_2) & 2\delta_3(1+2\delta_2)
\end{array}\right]\end{array}\tag{22}$$

where β_r is related to joint r.

Eq. (19) is solved with a fourth-order Runge–Kutta method to obtain the beam's deflection at different instants.

3. DET formulation for beams with breathing cracks

In general, two models are considered for breathing cracks. In the first one, the crack is assumed to be fully open or fully closed [7,10]. While the second model assumes that the crack opens and closes continuously [8,11]. There are experimental evidences that in reality the passage from closed to open crack and vice versa happens in a smooth way [8], the second model is used in this paper. Also, in the case of moving mass problem, using of first model for breathing cracks may lead to inaccurate results. Usually in moving mass problems, the beam deflection is often downwards and therefore, by using the first model, the crack at the bottom of the beam always remains open and the crack at the top of the beam remains closed all of the time. It means that if one assumes the crack at the bottom of the beam, the results from the first breathing model will be coincide with the results obtained from the case of open cracked beam. Also, if one assumes the crack at the top of the beam, the results will be coinciding with the results obtained from the case of no cracked beam even if a very deep crack is considered. These reasons lead to use of second breathing crack model here in which the crack opens and closes continuously.

Now, let us consider a beam with a breathing crack instead of an open crack. The formulation is the same as that in Section 2. However, here the coefficient β_j varies with time. The present work is different from other works reported in the literature with respect to breathing cracks. Previous papers considered a free or forced vibration with a known frequency. However, there is no known frequency to be used for determining β_j; hence, a different method must be explored. The simplest way to define β_j, such that it ranges from β_{j0} to 1 during the oscillation of the beam, is to define it as the ratio of instantaneous curvature to maximum curvature on the cracked element during motion. Based on the assumption that cracks have their maximal effect when y_j'', that is equal to

$$\left.\frac{\partial^2 y}{\partial x^2}\right|_{\text{at joint } j}$$

is maximum and regarding [11], stiffness may be expressed as follows:

$$k_j = k_{j0} + \frac{1}{2}(k_{\text{open}} - k_{j0})\left[1 + \frac{y_j''}{(y_j'')_{\max}}\right] \tag{23}$$

Here, k_{open} is the stiffness of the beam with a fully open crack and k_{j0} the stiffness with a fully closed one. Therefore, the coefficient β_j is determined from Eq. (7) as follows:

$$\beta_j = 1 + \frac{1}{2}(\beta_{j0} - 1)\left[1 + \frac{y_j''}{(y_j'')_{\max}}\right] \tag{24}$$

where β_{j0} is calculated from Eq. (8). Eq. (24) shows that when y_j'' is equal to $(y_j'')_{\max}$, β_j is minimum and equal to β_{j0} but when it is equal to $-(y_j'')_{\max}$, then β_j is maximum and equal to unity. It is important to note that the denominator depends on the properties of the excitation force such that it cannot be set *a priori* [8]. Since the maximum value of the curvature is unknown, it is initially obtained from a fully open crack problem. Having known the maximum curvature at crack location, the parameter β_j is calculated using Eq. (24) at each time instant. The matrix **A** is then calculated. The deflections of all points are determined by solving the system of differential equations (20). This process continued till the mass reaches to the end of the beam. The maximum curvature at crack location is recorded during the moving mass travelling. The problem now solves again with this new maximum curvature. This loop continues until the difference between the two last maximum curvatures becomes less than the value assumed.

4. FEM formulation for beams with cracks

For comparison of the results obtained from the two techniques, an FE code for beams without a crack and carrying moving mass was first developed and implemented in the MATLAB environment. The 2D beam elements have two nodes and four degrees of freedom as shown in Fig. 2.

Using the FE formulation, one easily can extract the stiffness and mass matrices of the beam element using the variational method [30]:

$$\mathbf{M_e} = \frac{mh}{420}\begin{bmatrix} 156 & 22h & 54 & -13h \\ 22h & 4h^2 & 13h & -3h^2 \\ 54 & 13h & 156 & -22h \\ -13h & -3h^2 & -22h & 4h^2 \end{bmatrix} \quad \mathbf{K_e} = \frac{EI}{h^3}\begin{bmatrix} 12 & 6h & -12 & 6h \\ 6h & 4h^2 & -6h & 2h^2 \\ -12 & -6h & 12 & -6h \\ 6h & 2h^2 & -6h & 4h^2 \end{bmatrix} \tag{25}$$

where A, h, EI are, respectively, the values for cross sectional, lengthwise, and flexural stiffness of the beam element.

Fig. 2. Finite element model of a 2D beam element.

After assembling the element matrices at each time step and taking the effects of Coriolis and centrifugal forces into account, the equation of motion for the entire system can be represented by

$$(\mathbf{M_b}+\mathbf{H_j})\ddot{\mathbf{y}}+\mathbf{C_j}\dot{\mathbf{y}}+(\mathbf{K_b}+\mathbf{K_j})\mathbf{y}=\mathbf{W_j}+\mathbf{P},\quad j=1,2,\ldots,n \tag{26}$$

where $\mathbf{M_b}$ and $\mathbf{K_b}$ are the beam mass and stiffness matrices, respectively. The right hand side vector $\mathbf{W_j}$ is the external force on the system and other matrices are defined as in Eq. (19). At this stage, the system governing equations will be solved by a fourth-order Runge–Kutta subroutine. The deflection of all nodes will be determined and will be used as initial conditions for the next time step. Note that as the position of the moving mass changes at each time step, the assembling process between beam and moving mass system needs to be repeated in order to calculate the whole system mass, stiffness, and damping matrices.

Now, if one assumes the open crack at the element r and considers Eq. (5), the matrix $\mathbf{K_e}$ for this element can be obtained as follows:

$$(\mathbf{K_e})_{\text{open}}=\mathbf{K_e}-\frac{D}{1+D\mathbf{K_e}\langle 4,4\rangle}(\mathbf{K_e}\langle :,4\rangle)(\mathbf{K_e}\langle 4,:\rangle) \tag{27}$$

where $\mathbf{K_e}\langle :,4\rangle$ and $\mathbf{K_e}\langle 4,:\rangle$ denote the fourth column and fourth row of matrix $\mathbf{K_e}$, respectively.

Employing the method used in Section 3, the matrix $\mathbf{K_e}$ for an element with a breathing crack can be calculated after some manipulation as

$$(\mathbf{K_e})_{\text{breathing}}=\mathbf{K_e}+\frac{1}{2}[(\mathbf{K_e})_{\text{open}}-\mathbf{K_e}]\left[1+\frac{y_j''}{(y_j'')_{\max}}\right] \tag{28}$$

5. Numerical example

A simply supported beam (Fig. 3) with the following characteristics is considered and an open crack is located in the middle of the beam [26]. Unless stated otherwise, all numerical results presented in this section are based on the following numerical data:

$$L=50\,\text{m},\quad E=2.1\times10^{11}\,\text{N}\,\text{m}^{-2},\quad I=0.0417\,\text{m}^4,\quad m=3930\,\text{kg}\,\text{m}^{-1},\quad m_p=39\,300\,\text{kg},\quad A=0.5\,\text{m}^2,$$

$$v=40\,\text{m}\,\text{s}^{-1},\quad g=9.81\,\text{m}\,\text{s}^{-2},\quad a/b=0.5,\quad L_c/L=0.5,\quad \text{height}=1.0\,\text{m},\quad \text{width}=0.5\,\text{m}$$

where L_c determines the location of the crack from the left hand side of the beam.

Table 1 presents the agreement between maximum deflection of the beam calculated in the present study and what has been proposed in Mahmoud and Abou-Zaid [26]. The technique they used is an approximate stationary mass approach recommended by Fryba [6] for light moving masses. It is notable that in their study, the terms for Coriolis and centrifugal forces are ignored.

The main idea in presenting Table 1 is to validate parts of our results against the available data. The differences between the results of [26] with ours are due to a number of factors including: (1) centrifugal force, (2) Coriolis force, and (3) the solution technique. In this numerical example, Coriolis force reduces the deflection of the beam while centrifugal force increases it. When both are taken into account, they somehow cancel out each other's effect. However, their cumulative effect may be very important for some other case studies.

In order to further investigate this matter, the effect of convective forces on the maximum normalized deflection of the beam with an open crack is illustrated in Table 2. As already mentioned, without taking into account the effects of inertia and centrifugal forces, the predicted results will be lower than the moving mass solution, i.e., when all the convective forces are accounted for. However, the effect of Coriolis force is in the opposite direction. By neglecting the effects of both terms of Coriolis and centrifugal forces, the result will be closer to the result obtained from all convective terms.

Fig. 4 shows the difference between the midpoint deflection of a beam with an open crack and the same beam with a breathing crack. In this figure, $T_0=L/v$ and is equal to the total time that the moving mass needs for one pass on the beam. The deflection-time response is normalized relative to the value $m_pgL^3/48EI$, which is the static deflection due to m_p at mid-span. It is seen that the difference between central point deflections of a beam without a crack and one with a fully

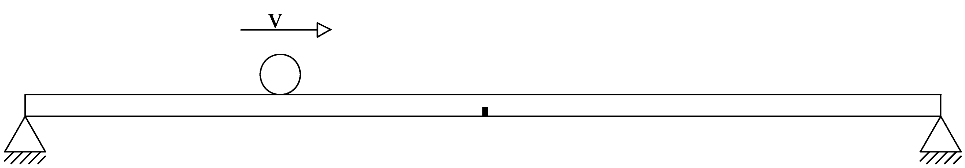

Fig. 3. Cracked simply supported beam with a moving mass.

Table 1
Maximum normalized deflection of an open cracked beam subjected to a moving mass.

Speed ($m\,s^{-1}$)	Maximum deflection [26]	Method	Maximum deflection (present study)	Difference (%)
10	1.34	DET	1.249	6.8
		FEM	1.288	3.9
20	1.43	DET	1.388	2.9
		FEM	1.411	1.3
40	2.13	DET	2.054	3.6
		FEM	2.046	3.9

Table 2
Maximum normalized deflection of an open cracked beam subjected to a moving mass with and without convective forces ($\nu = 40\,m\,s^{-1}$).

Moving mass (all convective terms)	Without inertia force	Without Coriolis force	Without centrifugal force	Without Coriolis and centrifugal forces
2.054	1.967 Error (−4.3%)	2.345 Error (14.6%)	1.840 Error (−10.4%)	2.095 Error (2.0%)

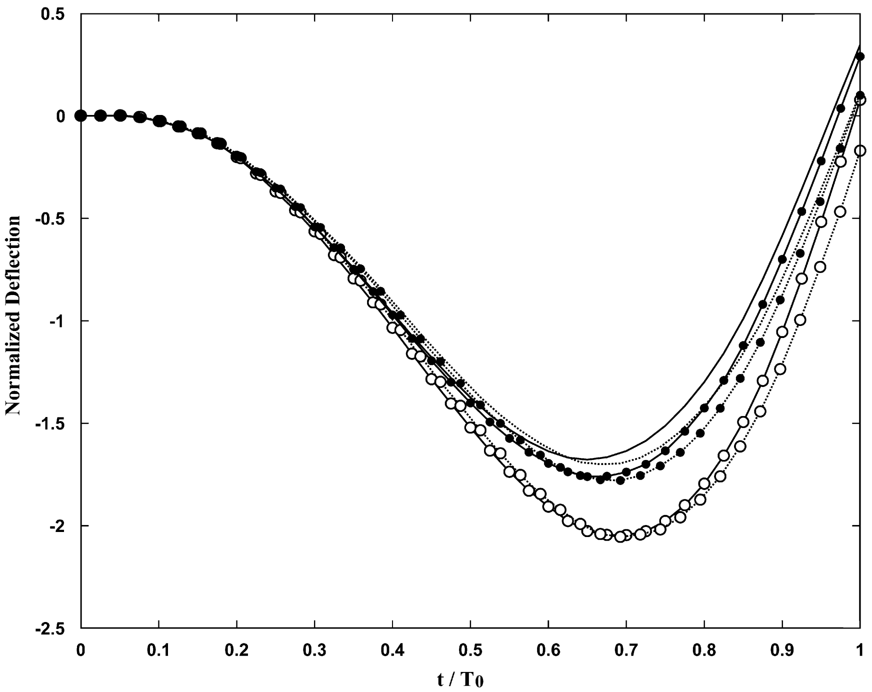

Fig. 4. Normalized deflection versus time at the mid-span of a simply supported beam subjected to open and breathing crack: ········ no crack using DET; ——— no crack using FEM; ·····○····· open crack using DET; ——○—— open crack using FEM; ·····●····· breathing crack using DET; and ——●—— breathing crack using FEM.

open crack is greater than that of the same beam and one with a breathing crack. It is also observed in this example that the central point deflection in a beam with a breathing crack is less than one with a fully open crack. This is because the stiffness value of a breathing cracked element varies between the same values for an element with an open crack and an uncracked one. The good agreement between the results of DET and FEM, and the saving in CPU time by using DET [19] lead to the utilization of DET technique for the next case studies.

In Fig. 5, the deflection-time response can be seen at mid-span for an open cracked beam and for different moving mass speeds with DET. As expected, an increase in velocity causes a corresponding increase in maximum dynamic deflection until a maximum value is reached. Thereafter, maximum deflection decreases even if the velocity continues to increase. The reason for this behaviour is the inability of the beam to respond fast enough to the excitation by the moving mass travelling at high velocity.

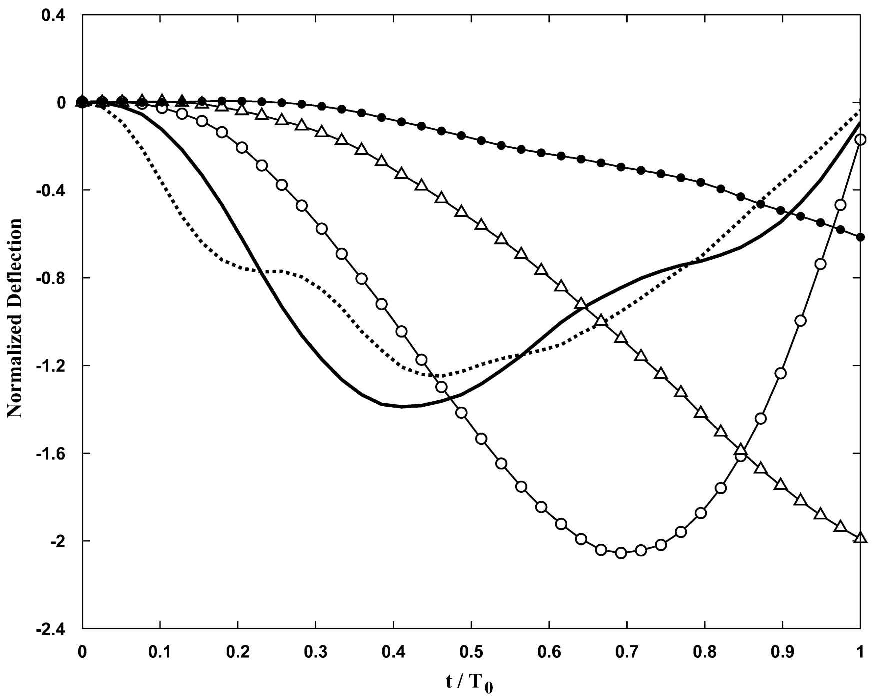

Fig. 5. Effect of the moving mass velocity on the time response at the mid-span of a simply supported beam: ········ $v = 10\,\mathrm{m\,s^{-1}}$; ——— $v = 20\,\mathrm{m\,s^{-1}}$; —○— $v = 40\,\mathrm{m\,s^{-1}}$; —△— $v = 80\,\mathrm{m\,s^{-1}}$; and —●— $v = 160\,\mathrm{m\,s^{-1}}$.

The effect of breathing crack location on the dynamic response was investigated in Fig. 6 by DET. It seems that increasing the distance of the crack location from the middle point of the simply supported beam, will decrease the beam midpoint deflection until it becomes nil at the two corners of the beam.

Fig. 7 shows the effect of the open and breathing crack size on the central deflection of the beam. In this example, it can be seen that by increasing the size of the crack, the midpoint deflection of the beam increases and this is more pronounced at larger values of a/b, specially for fully open cracks. Also, it can be observed that the effect of crack size in the case of breathing cracks can be different from the case with open cracks. The figure also demonstrates that despite the existence of a deep breathing crack in the middle of the beam, its effect on the beam deflection is not significant. This is due to the fact that the effective depth of a breathing crack varies from zero to its maximum during the beam deflection. Therefore, one may roughly estimates a breathing crack by an open crack with much smaller depth.

The difference between the first 20 natural frequencies of Euler–Bernoulli beams with and without a crack can be seen in Fig. 8. As this figure shows, for the case of $L_c/L = 0.5$, the anti-symmetric frequencies of the cracked and uncracked beams are equal. This is due to the fact that the crack is located at the node of the anti-symmetric modes for the simply supported beam. Also, the third, sixth, ninth … frequencies for the beam without a crack coincide with those of the beam with a crack at $L_c/L = 0.33$ for the same reason.

The effect of rotary inertia on the natural frequencies of the beam was also investigated using the DET (Fig. 9). When the height is small, the Euler–Bernoulli formulation is accurate enough. However, the effect of rotary inertia and shear deformation should be included in the formulation for greater heights.

Resonance vibrations have been observed on railway bridges subjected to high speed trains. Repeated action of axle loads at speeds reached on today's high speed lines can cause resonance. One group of these velocities can be obtained as [19,31]

$$v_{\mathrm{cr}} = \frac{d \times f_j}{k}, \quad k = 1, 2, 3, \ldots \tag{29}$$

where d is the distance of each two moving forces and f_j the jth natural frequency of the beam. If one takes d to be equal to L, the first critical velocity related to the first natural frequency is obtained as follows [19]:

$$v_{\mathrm{cr}} = L \times f_1 \tag{30}$$

Let us now investigate the effect of several moving forces using the same beam geometry. A new load is assumed to enter the beam domain from the left as soon as the old one exits from the right, the process being repeated for an arbitrary number of times. The transient effects due to previous loads are required to be included in this case, a requirement that does not apply to studies with single loads. In Figs. 10 and 11, the normalized midpoint deflection of the beam is plotted against the normalized time for the beam with open, breathing, or no crack and for two different moving load velocities,

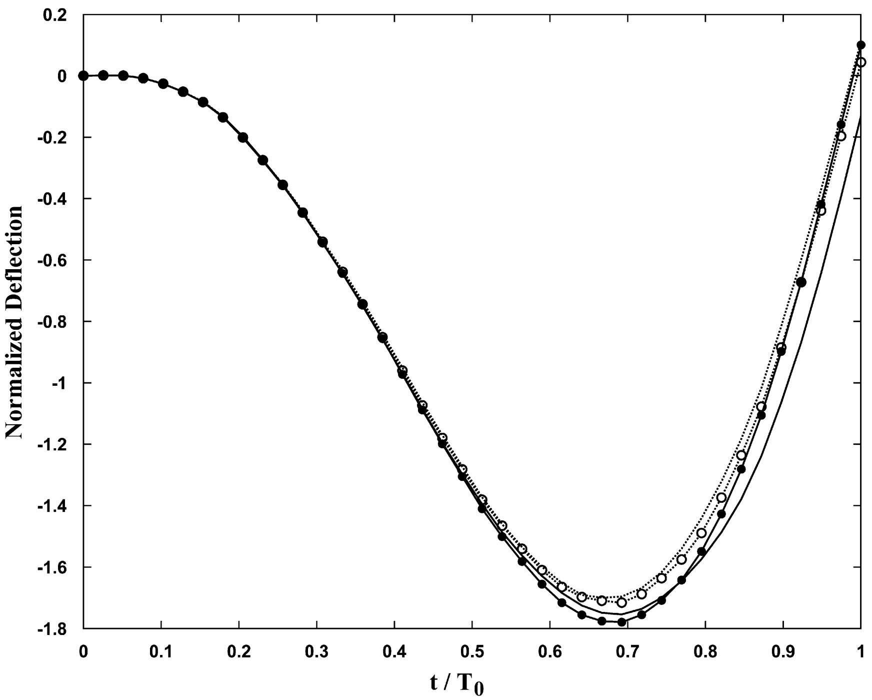

Fig. 6. Effect of breathing crack location on the time response at mid-span (moving mass speed $= 40\,\mathrm{m\,s^{-1}}$): ········ no crack ($L_c/L = 0.0$ or 1.0); ·····○····· $L_c/L = 1/4$; ——— $L_c/L = 3/4$; and ——●—— $L_c/L = 1/2$.

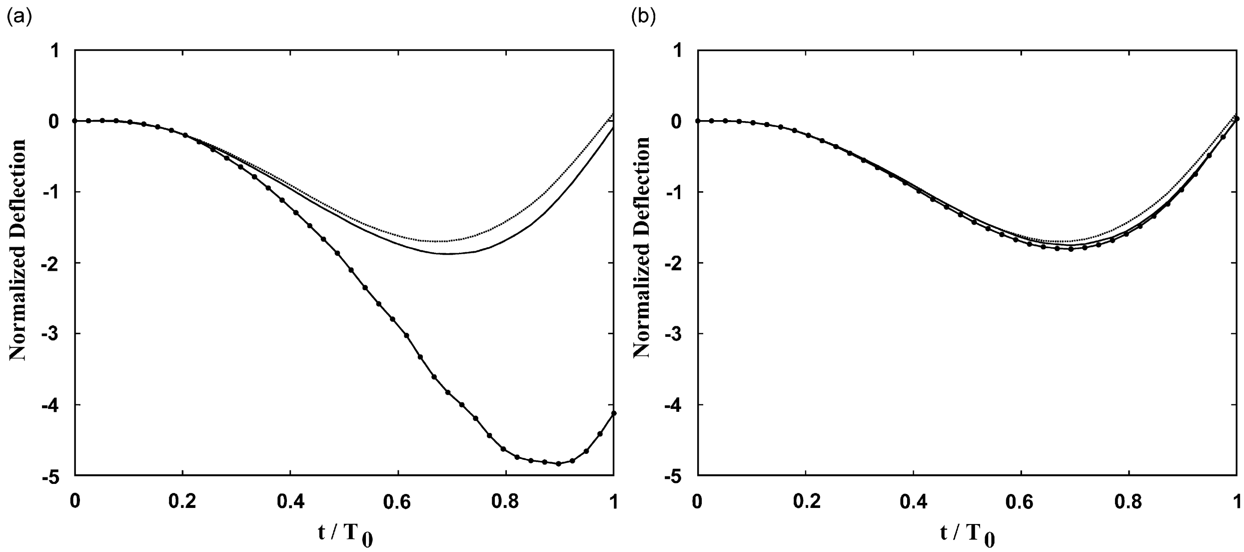

Fig. 7. Effect of crack size on the time response at the mid-span of a simply supported beam; (moving mass speed $= 40\,\mathrm{m\,s^{-1}}$, $L_c/L = 1/2$): (a) fully open crack: ········ $a/b = 0.0$; ——— $a/b = 0.4$; ——●—— $a/b = 0.8$ and (b) breathing crack: ········ $a/b = 0.0$; ——— $a/b = 0.4$; ——●—— $a/b = 0.8$.

namely, 30 and $46\,\mathrm{m\,s^{-1}}$. At a speed of $30\,\mathrm{m\,s^{-1}}$ which is not a critical speed, resonance cannot be observed for beams with or without cracks. In this figure, the deflection amplitude of the beam with an open crack is always larger than the beam without a crack. A speed of $46\,\mathrm{m\,s^{-1}}$ is one critical speed for the beam without a crack ($\upsilon_{\mathrm{cr}} = L \times f_1$ for $L = 50\,\mathrm{m}$ and $f_1 = 0.938\,\mathrm{Hz}$). Although a clear resonance is observable in the response of the uncracked beam, the responses of beams with open and breathing cracks are bounded and exhibit the beating phenomenon. This means that the existence of crack can shift the critical velocity that causes the resonance in the beam. This shift is larger for the beam containing an open

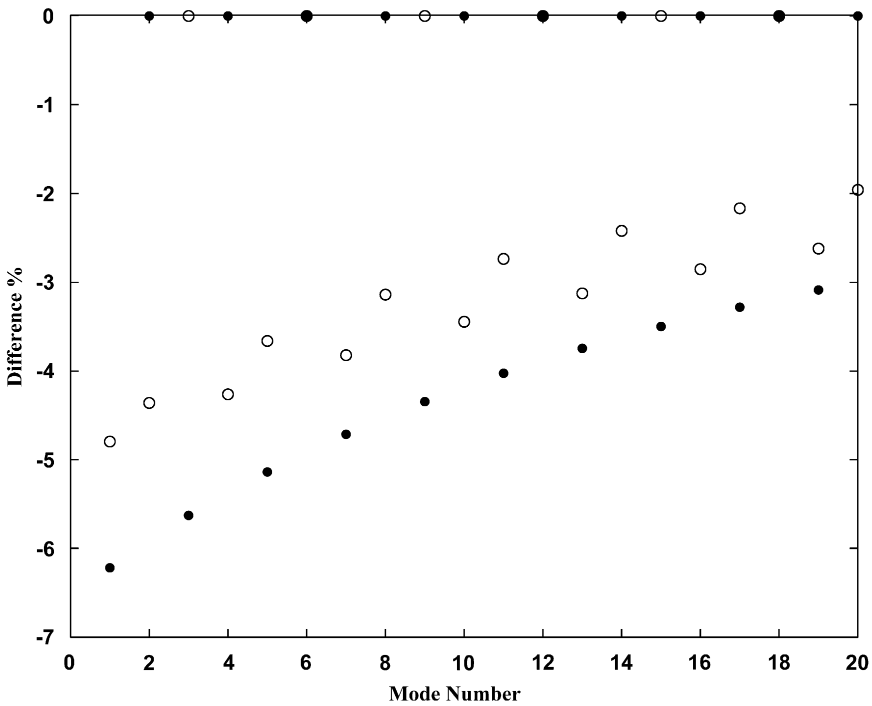

Fig. 8. Percentage of difference between natural frequencies of the beam with and without fully open crack (height = 1.0 m, width = 0.5 m, $a/b = 0.5$) (Difference (%) $= \frac{\text{Natural frequency (with crack)} - \text{Natural frequency (without crack)}}{\text{Natural frequency (without crack)}} \times 100$): ● $L_c/L = 0.5$; ○ $L_c/L = 0.33$.

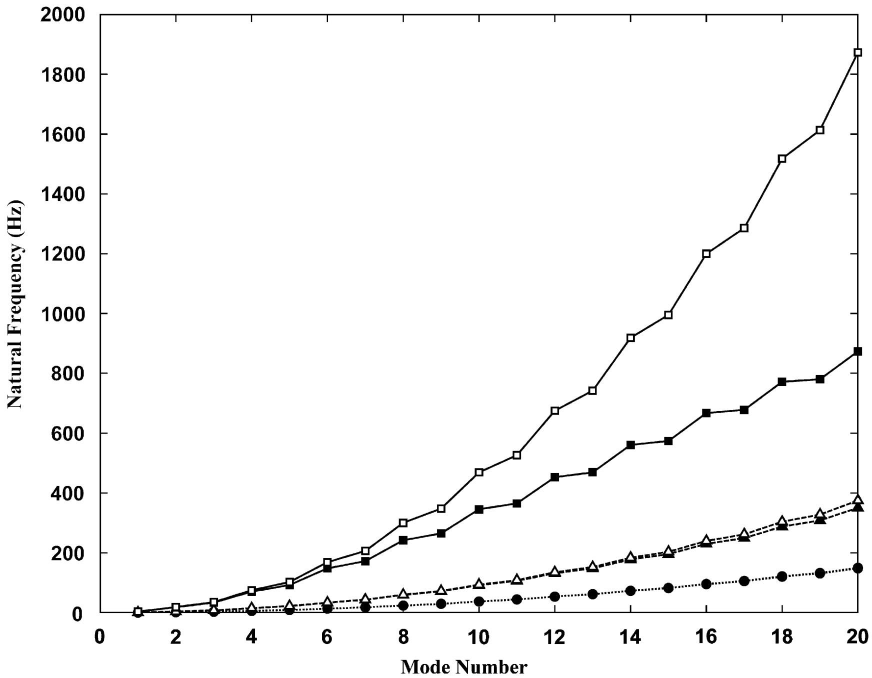

Fig. 9. Effect of rotary inertia on the natural frequencies of a simply supported beam with fully open crack using DET ($L_c/L = 0.5$, $a/b = 0.5$): with rotary inertia: ⋯●⋯ height = 0.4 m; - - -▲- - - height = 1.0 m; —■— height = 5.0 m and without rotary inertia: ⋯○⋯ height = 0.4 m; - - -△- - - height = 1.0 m; —□— height = 5.0 m.

crack. The first critical speeds for the beam with open and breathing cracks are 43.2 and 44.6 $\mathrm{m\,s^{-1}}$, respectively. For this reason, the response amplitude of the beam with an open crack is lower than that in the beam with a breathing crack.

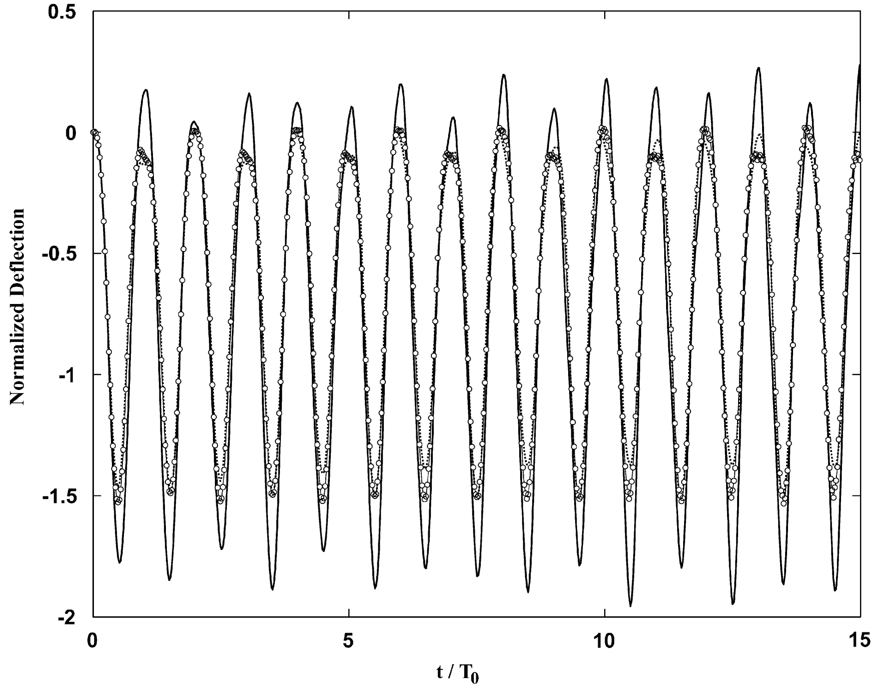

Fig. 10. Midpoint beam deflection as a function of time for the moving mass speed = 30 $m\,s^{-1}$: ········ no crack; ———— open crack; and —○— breathing crack.

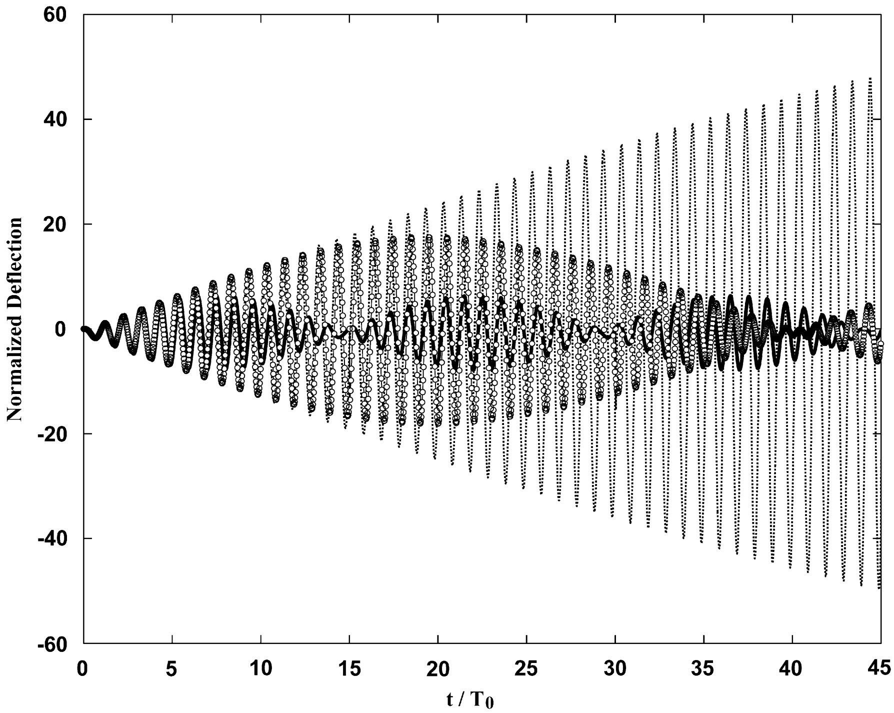

Fig. 11. Midpoint beam deflection as a function of time for the moving mass speed = 46 $m\,s^{-1}$: ········ no crack; ———— open crack; and —○— breathing crack.

6. Conclusions

- A discrete element technique and a finite element method formulation were presented for beams with cracks carrying moving masses. In DET, continuous flexible beam elements are replaced with a system of rigid bars and flexible joints. The main characteristic of the technique in comparison with other methods is ease of programming.

- The formulation of a beam with breathing cracks was presented. The formulation is the same as that for a fully open crack with differences in the value of coefficient β_j varying with time. It was found that the beam with a breathing crack has less deflection compared with the fully open cracked beam.
- The effect of the moving load velocity on the beam deflection was also investigated. It was found that by increasing the velocity, the maximum dynamic deflection will increase until a critical velocity was reached. After that critical velocity, the maximum deflection will be decreased. This is due to the fact that the beam cannot respond fast enough to high-velocity excitation.
- It was observed that moving the location of the crack towards the central point of the beam and also increasing crack depth will increase its effect for a beam with open and breathing cracks.
- Some natural frequencies of the cracked beam were compared with one without it. It was found that for the simply supported beam with midpoint crack, the anti-symmetric frequencies have a good agreement with a beam without crack because of the existence of a node in the central point of the beam for anti-symmetric modes.
- Finally, the effect of crack on the resonance of the beam was investigated. It was seen that the crack can change the critical velocity leading to the resonance of the beam.

Appendix A

In this Appendix, the effects of Coriolis and centrifugal forces are added to DET formulation. Neglecting the effects of these forces, the equation of motion will be obtained at each time instant in matrix form as [18]

$$(\mathbf{Q}+\mathbf{H})\mathbf{Y}_{,\mathbf{tt}}+\mathbf{AY}=\mathbf{W}+\mathbf{P} \tag{A.1}$$

Let us first consider Eq. (16) which only takes into account the inertia force. By replacing this equation to Lagrange's equations, for example in jth time instant, one can obtain

$$\frac{\mathrm{d}}{\mathrm{d}t}\left\{\frac{\partial\left[\frac{1}{2}m_p\left(\frac{\mathrm{d}y_j}{\mathrm{d}t}\right)^2\right]}{\partial\dot{y}_j}\right\}+\frac{\partial\left[\frac{1}{2}m_p\left(\frac{\mathrm{d}y_j}{\mathrm{d}t}\right)^2\right]}{\partial y_j}=m_p\ddot{y}_j$$

$$\frac{(2j-1)L}{2nv}<t_j<\frac{(2j+1)L}{2nv},\quad j=1,2,\ldots,n-1 \tag{A.2}$$

In the above term, the kinetic energy related to the moving mass speed is neglected. By considering the general term for the kinetic energy of the moving mass, the right hand side of Eq. (A.2) is substituted by

$$\frac{\mathrm{d}}{\mathrm{d}t}\left[\frac{\partial T_{\mathrm{II}}}{\partial\dot{y}_j}\right]+\frac{\partial T_{\mathrm{II}}}{\partial y_j}=m_p\left(\ddot{y}_j+2\omega_j v+\frac{v^2}{R}\right)=m_p(\ddot{y}_j+2\dot{y}_j'v+y_j''v^2)$$

$$\frac{(2j-1)L}{2nv}<t_j<\frac{(2j+1)L}{2nv},\quad j=1,2,\ldots,n-1 \tag{A.3}$$

In Eq. (A.3), the over dot $(\cdot)$ denotes the differentiation with respect to time t and the right prime $(')$ denotes the differentiation with respect to the local coordinate x. The term $m_p(v^2/R)$ represents the centrifugal force. The parameter R in this equation is the curvature radius of the beam at the moving mass location. Note that the inverse of beam curvature is equal to y_j''. The terms $m_p\ddot{y}_j$ and $2m_p\omega_j v$, respectively, represent the inertia force and Coriolis force. The angular velocity of jth element, ω_j, in Coriolis term is equal to $\dot{y}_j'$ and can be written as

$$\dot{y}_j'=\frac{1}{h}(\dot{y}_j-\dot{y}_{j-1}) \tag{A.4}$$

Also, $1/R$ in centrifugal force term is equal to y_j'' for small deflections and is expressed as

$$y_j''=\frac{1}{h^2}(y_{j+1}+y_{j-1}-2y_j) \tag{A.5}$$

After some manipulations, Eq. (A.1) is converted to

$$(\mathbf{Q}+\mathbf{H})\mathbf{Y}_{,\mathbf{tt}}+\mathbf{C}\mathbf{Y}_{,\mathbf{t}}+(\mathbf{A}+\mathbf{K})\mathbf{Y}=\mathbf{W}+\mathbf{P} \tag{A.6}$$

Note that matrices **C** and **K** are time dependent and obtained from Eqs. (A.7) and (A.8), respectively.

$$\mathbf{C}_1=\frac{2vm_pn}{L}\begin{bmatrix} 1 & 0 & & & \\ 0 & 0 & 0 & \ldots & \\ & 0 & 0 & \ldots & \\ & \ldots & \ldots & \ldots & \\ & & & & \\ & & & & \end{bmatrix},\quad \mathbf{C}_2=\frac{2vm_pn}{L}\begin{bmatrix} 0 & 0 & & & \\ -1 & 1 & 0 & \ldots & \\ & 0 & 0 & \ldots & \\ & \ldots & \ldots & \ldots & \\ & & & & \\ & & & & \end{bmatrix},\ldots,$$

$$\mathbf{C_n}=\frac{2vm_pn}{L}\begin{bmatrix} 0 & 0 & & & & & & \\ 0 & 0 & 0 & \ldots & & & & \\ & 0 & 0 & \ldots & & & & \\ & \ldots & \ldots & \ldots & & & & \\ & & & & & & & \\ & & & & & 0 & 0 & \\ & & & & 0 & 0 & 0 & 0 \\ & & & & & 0 & -1 & \delta_3 \end{bmatrix} \tag{A.7}$$

$$\mathbf{K_1}=-\frac{m_pv^2n^2}{L^2}\begin{bmatrix} 2 & -1 & 0 & & \\ 0 & 0 & 0 & \ldots & \\ & 0 & 0 & \ldots & \\ & \ldots & \ldots & \ldots & \\ & & & & \\ & & & & \end{bmatrix},\quad \mathbf{K_2}=-\frac{m_pv^2n^2}{L^2}\begin{bmatrix} 0 & 0 & & & \\ -1 & 2 & -1 & \ldots & \\ & 0 & 0 & \ldots & \\ & \ldots & \ldots & \ldots & \\ & & & & \\ & & & & \end{bmatrix},\ldots,$$

$$\mathbf{K_n}=-\frac{m_pv^2n^2}{L^2}\begin{bmatrix} 0 & 0 & & & & & & \\ 0 & 0 & 0 & \ldots & & & & \\ & 0 & 0 & \ldots & & & & \\ & \ldots & \ldots & \ldots & & & & \\ & & & & & & & \\ & & & & \ldots & \ldots & 0 & 0 \\ & & & & \ldots & 0 & 0 & 0 \\ & & & & 0 & 0 & -1 & 2\delta_3 \end{bmatrix} \tag{A.8}$$

Visualization of second and third terms in right hand side of Eq. (A.3) is considered in Fig. A1. The angular velocity of the element subjected to the moving mass leads to Coriolis force acted on the beam (Fig. A1(a)). However, by considering rigid bars instead of flexible elements, the curvature on the rigid bars is

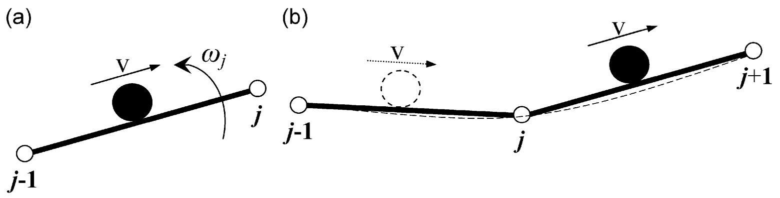

Fig. A1. Creation of convective forces due to relative velocity between the beam and the moving mass: (a) Coriolis force and (b) centrifugal force.

zero while at the joints is infinite (Fig. A1(b)). For this reason, two adjacent rigid bars are considered and the average curvature for them is computed by Eq. (A.5) which is the similar to the one normally used in FEM.

References

[1] G.G. Stokes, Discussion of a differential equation relating to the breaking of railway bridges, *Transactions of the Cambridge Philosophical Society* 85 (5) (1849) 707–735.
[2] R. Willis, *Commissioners Report: Application of Iron to Railway Structures*, William Clowes & Sons, London, 1849.
[3] R.S. Ayre, G. Ford, L.S. Jacobsen, Transverse vibration of a two span beam under the action of a moving constant force, American Society of Mechanical Engineers Transactions, *Journal of Applied Mechanics* 17 (1950) 1–12.
[4] C.E. Inglis, *A Mathematical Treatise on Vibration in Railway Bridges*, Cambridge University Press, Cambridge, 1934.
[5] A. Hilderberg, *Dynamic Influences of Smoothly Running Loads on Simply Supported Girders*, Kungl Tekniska Hogskolan, Stockholm, Sweden, 1951.
[6] L. Fryba, *Vibration of Solids and Structures Under Moving Loads*, Telford, London, 1999.
[7] S.M. Cheng, A.S.J. Swamidas, X.J. Wu, W. Wallace, Vibrational response of a beam with a breathing crack, *Journal of Sound and Vibration* 225 (1) (1999) 201–208.
[8] N. Pugno, C. Surace, Evaluation of the non-linear dynamic response to harmonic excitation of a beam with several breathing cracks, *Journal of Sound and Vibration* 235 (5) (2000) 749–762.
[9] M. Kisa, J. Brandon, The effects of closure of cracks on the dynamics of a cracked cantilever beam, *Journal of Sound and Vibration* 238 (1) (2000) 1–18.
[10] T.G. Chondros, A.D. Dimarogonas, J. Yao, Vibration of a beam with a breathing crack, *Journal of Sound and Vibration* 239 (1) (2001) 57–67.
[11] E. Douka, L.J. Hadjileontiadis, Time–frequency analysis of the free vibration response of a beam with a breathing crack, *NDT&E International* 38 (2005) 3–10.
[12] A.P. Bovsunovsky, C. Surace, Considerations regarding super harmonic vibrations of a cracked beam and the variation in damping caused by the presence of the crack, *Journal of Sound and Vibration* 288 (2005) 865–886.
[13] O.N.L. Abraham, J.A. Brandon, Remark on the determination of compliance coefficients at the crack section of a uniform beam with circular cross-section, *Journal of Sound and Vibration* 169 (1994) 570–574.
[14] J.E. Akin, M. Mofid, Analytical numerical solution for response of beams with moving mass, *ASCE Journal of Structural Engineering* 115 (1) (1989) 120–131.
[15] M. Mofid, J.E. Akin, Discrete element response of beams with traveling mass, *Advances in Engineering Software* 25 (2–3) (1996) 323–331.
[16] M. Mofid, Discrete element model for beams on elastic foundation, *Proceedings of Kerensky International Conference*, Kuala Lumpur, Malaysia, 1994.
[17] M. Mofid, M. Shadnam, On the response of beams with internal hinges under moving mass, *Advances in Engineering Software* 31 (2000) 323–328.
[18] A. Yavari, M. Nouri, M. Mofid, Discrete element analysis of dynamic response of Timoshenko beams under moving mass, *Advances in Engineering Software* 33 (2002) 143–153.
[19] S. Ziaei-Rad, A. Ariaei, M. Imregun, Vibration analysis of Timoshenko beams under uniform partially distributed moving masses, *Journal of Multi-body Dynamics* 221 (2007) 551–566.
[20] A.D. Dimarogonas, Vibration of cracked structures—a state of the art review, *Engineering Fracture Mechanics* 55 (1996) 831–857.
[21] E.I. Shifrin, R. Ruotolo, Natural frequencies of a beam with an arbitrary number of cracks, *Journal of Sound and Vibration* 222 (1999) 409–423.
[22] J. Kuang, B. Huang, The effect of blade crack on mode localization in rotating bladed disks, *Journal of Sound and Vibration* 227 (1999) 95–103.
[23] N. Pugno, C. Surace, R. Ruotolo, Evaluation of the non-linear dynamic response to harmonic excitation of a beam with several breathing cracks, *Journal of Sound and Vibration* 235 (2000) 749–762.
[24] D.R. Parhi, A.K. Behera, Dynamic defection of a cracked shaft subjected to moving mass, *Transactions of the CSME* 21 (1997) 295–316.
[25] M.A. Mahmoud, Stress intensity factors for single and double edge cracks in a simple beam subject to a moving load, *International Journal of Fracture* 111 (2001) 151–161.
[26] M.A. Mahmoud, M.A. Abou Zaid, Dynamic response of a beam with a crack subject to a moving mass, *Journal of Sound and Vibration* 256 (2002) 591–603.
[27] H.-I. Yoon, I.-S. Son, Dynamic behaviour of cracked simply supported pipe conveying fluid with moving mass, *Journal of Sound and Vibration* 292 (2006) 941–953.
[28] C. Bilello, L.A. Bergman, Vibration of damaged beams under a moving mass: theory and experimental validation, *Journal of Sound and Vibration* 274 (2004) 567–582.
[29] J.J. Wu, Vibration analyses of a portal frame under the action of a moving distributed mass using moving mass element, *International Journal of Numerical Methods and Engineering* 62 (2005) 2028–2052.
[30] O.C. Zienkiewicz, R.L. Taylor, The Finite Element Method, fourth ed., Vol. 1, 1988, McGraw-Hill, New York.
[31] L. Fryba, A rough assessment of railway bridges for high speed trains, *Engineering Structures* 23 (2001) 548–556.